International Journal of Trend in Scientific Research and Development (IJTSRD)
Volume 6 Issue 3, March-April 2022 Available Online: www.ijtsrd.com e-ISSN: 2456 – 6470

Mechanical and Structural Properties of Eastern Nigeria Tortoise Shell

Damian Okechukwu Okongwu[1], Sylvester Emeka Abonyi[2], Anthony Amaechi Okafor[3]

[1]Department of Production Engineering, Nnamdi Azikiwe University Awka, Anambra State, Nigeria
[2]Department of Electrical Engineering, Nnamdi Azikiwe University Awka, Anambra State, Nigeria
[3]Department of Mechanical Engineering Nnamdi Azikiwe University Awka, Anambra State, Nigeria

ABSTRACT

Macro-structural and mechanical properties of tortoise shells of Nigeria indigenous specie were studied to reveal its evolution as a natural load-bearing protective amour. The shell is revealed in this study to be a natural sandwich composite made of keratin, dorsal cortex, porous bone and ventral cortex. Indications of delamination which help the tortoise to absorb shocks were seen in the keratin. The dorsal and ventral cortexes were seen to be load bearing members with distribution of fibers in a manner that sustain dead load. The porosity seen in the middle porous layer ensures that the carapace is not too heavy for the tortoise to carry thus guarantees ease of locomotion, strength and damping. The average porosity of the studied shells is determined to be 31.0425% which as expected is smaller than the value 48.9% reported for porosity of shell of the turtle Terrapene Carolina in literature. The suture of the shell is revealed to house a zigzag interlocking design that allow slight deformation of the shell under light loads required for respiration, locomotion and metabolism but stiffen under excessive deformation. Stiffness of two specimens was determined to be $k = 1.4907 \times 10^{-6} NM^{-1}$ and $k = 1.1232 \times 10^{-6} NM^{-1}$ for the shells with masses 0.2362 kg and 0.2764Kg respectively. These stiffness values were as expected higher the typical values for those of turtles. The stiffness to mass ratio(k/m) for the two shells were respectively calculated to be $6.3112 \times 10^{-6} NM^{-1}kg^{-1}$ and $4.0637 \times 10^{-6} NM^{-1}kg^{-1}$. The conditions established for equivalent synthetic shells to have less stiffness to mass ratio were $\rho \rangle 7.2177 \times 10^{6} kg^{-3}$ and $\rho \rangle 6.3457 \times 10^{6} kg^{-3}$ respectively. These conditions were shown not to be because of problems of stress concentration and weakness at the joints and delamination of the biological shells.

KEYWORDS: *Tortoise Shell, metabolism, deformation, Stiffness*

How to cite this paper: Damian Okechukwu Okongwu | Sylvester Emeka Abonyi | Anthony Amaechi Okafor "Mechanical and Structural Properties of Eastern Nigeria Tortoise Shell" Published in International Journal of Trend in Scientific Research and Development (ijtsrd), ISSN: 2456-6470, Volume-6 | Issue-3, April 2022, pp.678-686, URL: www.ijtsrd.com/papers/ijtsrd49532.pdf

IJTSRD49532

1. INTRODUCTION

Turtles which belong to the family of testudines with tortoises haven evolved for about quarter of a billion years (Triassic period of the Mezozoic era) [1-3]. Turtles and tortoises are very slow and peaceful reptiles that suffer predation from faster animals like ravens, raccoons, and coyotes, alligators, crocodiles and tiger sharks. In a bid to survive these predators they have evolved protective armor [4] called shells which they carry along to shelter them from danger during attack.

The shell provides protection by providing a space for the whole body to retract when threatened. The shape, structural strength and material strength of the carapace protect the turtle from wounds, flipper amputation, tooth marks, bites [5].

More specific kinds of predatory attacks suffered by turtles are nibbling at the edges of the shell or poking into soft or thin parts of the shell or carapace by ravens, raccoons, and coyotes [6, 7]

and crushing of the protective shell with great jaw force by alligators, crocodiles and tiger sharks [8-10]. These recognized attacks undoubtedly mean that turtle shells evolved to resist compressive loads of predatory attacks. This hypothesis has been tested to be true in [11] in which it is shown that shell thickness (which predominantly influence shell strength) and bite force of predators evolved in parallel. The shell acts as anchoring frame for the muscles [12, 13] thus is essential for locomotion and respiration. The shell serves as major store of mineral to the body [14] and also serves as reservoir of water and functions as a pH buffer [15, 16]. The shell is a natural sensor in turtles for vibration and tactile perception [17]. Tortoise/turtle shell is also designed by nature to be dissipative of impact loading while distributing the internal stress effectively without fracture [18]. The shell of the turtle is composed mainly of keratin and rough scales called scutes that add to the strength of the shell [19-21]. Bio-mimicking the multi-scale structure existing in natural creations like tortoise shells provide ideas for engineered multi-functionality [22, 23]. Hence, it becomes important to evaluate the mechanical properties arising because of different sandwich layers of eastern Nigeria tortoise shell which remain largely unstudied.

2. Materials and methods

Mature specimens were tested with the universal testing machine stationed at the Standards Organization of Nigeria (SON) Enugu. The steps followed are; the movable jaw is brought to the position so as to fix the sample between the two jaws. The *start compression test key* is pressed and the movable jaw moves towards the fix jaw, thus compressing the sample. The load on the test sample is displayed and the length travelled by the movable jaw is also displayed. Compression stops after failure. The machine is programmed to sense failure and stop compression when load drops below the cut-off percent of the peak load. The results of compression tests are stored in the compression memory and then printed. Specimen is detached from the carapace for micro-structural examination. The micro-structural examination is intended for through-the-thickness surface of the specimen along a longitudinal plane.

The available instrument for preliminary observation is an optical microscope (L2003A Reflected Light Metallurgical Microscope) in the metallurgical laboratory of the *Metallurgical Training Institute* in Onitsha, Nigeria. The examined surface is made long enough to include the suture between two ribs. After setting and powering the microscope, the detached specimen was staged on it and the surface of interest examined through the *eyepiece* without any preparation. Nothing was revealed due to very poor contrast amongst different structural configurations of the surface. The surface is then prepared by grinding with dark emery paper (P400C Water Proof Silicon Carbide Paper). This preparation helped to darken the porous depressions of the examined surface and also helped to make the examined surface perpendicular to the microscopic illumination in order to avoid parallax error. After this preparation some of the different structural configurations of the through-the-thickness direction of the examined surface got revealed by the microscope as the *stage* is moved with the *cross knob* while inter-rib suture with interlocking design is revealed when the examined surface is moved longitudinally with the *lengthwise knob*. The observed microstructures are snapped with a digital camera through the *trinocular* and saved for use.

Synthetic spherical structural shell with isotropic material and mechanical property distribution is expected to fail in a different manner from a natural multi-scale sandwich composite shell. The naturals and wich composite shell like tortoise shell is hierarchical in nature and thus made of different multi-scale constituents which are linked and bonded at joints. When such shell is loaded quasi-statically, the most affected constituent or joint will fail with crack ensuing slowly in the weakest direction. The homogeneous synthetic counterpart will not fail with such behavior but will deform and fail in the neighborhood of the applied force. If the synthetic counterpart is brittle, failure will be in the form of crack initiation and catastrophic growth to sudden failure.

The nature of deformation of spherical shell as discussed by Steele [24] is shown in figure 1 below.

The graphic model depicts that a loaded shell suffers a dimpled deformation. A point load F acts on an isotropic spherical dome of uniform thickness t, diameter D. Considerations leading to figure 1 supposes that the shell is sufficiently stiff. The angular position of the edge of the inverted cap normally lies in the range $\alpha\langle 0.3$ with respect to the vertical. The edge of the spherical cap suffers stress concentration and normally becomes the line of failure.

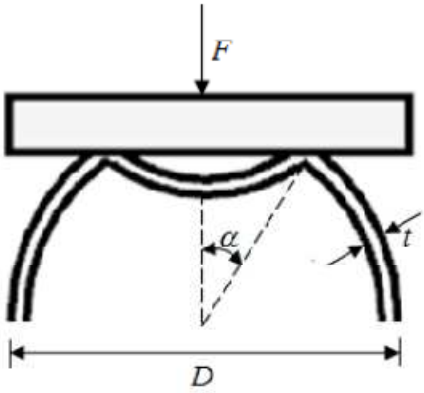

Figure 1 The nature of deformation of spherical shell as discussed by Steele [24]

Assuming that the force F is within the elastic range (that is, F is of order of magnitude such that when removed the shell recovers from cap inversion) then the stiffness of the shell becomes

$$k = \frac{F}{\delta} \qquad (1)$$

The symbol δ stands for deformation which is seen from geometric consideration of figure 1 to be given by

$$\delta = \frac{D}{2}(1-\cos\alpha) \qquad (2)$$

By linear expansion, the elastic potential energy associated with the deformation in figure 1 is

$$U(\alpha) = 2\pi Etc^2\sqrt{\frac{D}{2}\alpha^3 - \frac{1}{4}FD\alpha^2} \qquad (3)$$

Where c is the reduced thickness given by

$$C = \frac{1}{\sqrt{12(1-v^2)}} \qquad (4)$$

The deformation in figure 1 forms such that takes value that provides minimum potential energy for agiven force F. Then minimization means

$$\frac{\partial}{\partial\alpha}U(\alpha) = 6\pi Etc^2\sqrt{\frac{D}{2}\alpha^2 - \frac{1}{2}FD\alpha} = 0 \qquad (5)$$

It seen that the roots of equation (5) are

$$\alpha_1 = 0 \qquad (6a)$$

$$\alpha_2 = \frac{FD}{12\pi Etc^2\sqrt{D/C}} \qquad (6b)$$

It is seen that the solution $\alpha_1 = 0$ will give infinite value for k when inserted in equation (7) thus it isnot feasible and discarded. The feasible solution then becomes $\alpha_2 = \frac{FD}{12\pi Etc^2\sqrt{D/C}}$ meaning that in light ofequations (2 & 6b) equation (1) becomes

$$k = \frac{2F}{D\left(1-\cos\left[FD/\left\{12\beta\pi Etc^2\sqrt{D/C}\right\}\right]\right)} \qquad (7)$$

Equation (7) is rearranged to become

$$kD\left(1-\cos[FD/\left\{12Etc^2\sqrt{D/C}\right\}\right) - 2F = 0 \qquad (8)$$

Equation (8) is a transcendental equation in D that could be very challenging to solve. The aim of analysis in this section is to ascribe the values of the parameters; $k, F, E, t \text{ and } C$ and as experimentally determined for the tortoise shell to the equivalent spherical dome and then compute the diameter D of the equivalent spherical dome that offer same resistance k to external force F. Making use of equation (4)leads to equation (8) becoming

$$kD\left(1-\cos[FD/\left\{12Etc^2\sqrt{D/C}\right\}\right) - 2F = 0 \qquad (9)$$

The values of $E \text{ and } v$ for tortoise shell being a natural multi-scale structure are difficult to determinebut the work of Panakkal et al, [25] offers a way to handle this problem. Panakkal et al, [25] proposedmodels for elastic properties of porous materials. The model they proposed for porous elastic modulus Ebased on the dense parent material elastic modulus $E_0$is as follows

$$E = E_0 e^{\left(-b\theta - c\theta^2\right)} \qquad (10)$$

Where θ the porosity and b and c are constants that are determined experimentally. Based on the work of Panakkal et al, [25], Gibson and Ashby [26] proposed a model for the Poisson's ratio of porous material in terms of dense parent material and porosity as

$$v = v_0(1-d\theta) \qquad (11)$$

Where d is a constant that is determined experimentally. Equations (10) and (11) are inserted in equation(9) to give

$$kD\left(1-\cos\left[\frac{12^{0.75}FD\left[0.5\right]\left[1-v^2{}_0(1-d\theta)^2\right]^{.75}}{12\pi E_0 e^{\left(-b\theta-c\theta^2\right)}t^{2.5}}\right]-2F\right) = 0 \qquad (12)$$

Equation (12) is the proposed equation for computation of equivalent structural dome. Equation (12) has a transcendental nature and very difficult to solve analytically. Newton-Raphs on and bisection method are among the available interpolation techniques available for their solution.

MATLAB program that implements solution search will be used to solve equation (12).

A pertinent question to ask is how important computation of equivalent structural spherical dome as being presented in the ongoing section is. Such a computation could become a new procedure for judging natural optimization of tortoise shell as a load bearing structure. For example natural optimization of tortoise shell will be inferred if its stiffness to weight ratio is greater than that of equivalent synthetic spherical dome.

3. Results and discussion Physical features of shells

The upper part of the shell called Carapace and the lower part called plastron are strongly connected by a bonny bridge placed between the fore and hind limbs. The shell is seen to exhibit some kind of longitudinal symmetry when cut along the vertebral line indicated green in figure 2a. This line of symmetry is naturally revealed in the ventral view of the plastron as indicated with an arrow in figure2b.The bridge in the studied specie is part of the plastron and cements with the carapace. A sketch of the dorsal view of carapace of the studied tortoise species is shown in figure 3a to have 24 peripheral plates surrounding 13 main carapacial plates. Five of the main carapacial plates are cantered along the midvertebral line while four each are symmetrically placed on both sides of the mid-plates. The physicalmorphology of carapace of emydid turtle as adapted from the work [27] is also shown in figure 3b for comparison. It is seen that though the carapace of emydid turtle has same number of main carapacialplates as the studied carapace, it has one more peripheral plate than the studied carapace.

A sketch of the ventral view of plastron of the studied tortoise specie is shown in figure 4a to have 12 plates. A sketch of plastron of emydid turtle as adapted from the work [27] is shown in figure 4b for comparison. It should benoted that the studied plastron has same number of plates as the emydid turtle. The main difference between the two is that the most anterior and the most posterior plates are smaller in size relative to other plastral plates in the studied plastron than in the plastron of the emydid turtle. A carapacial hinge (indicated with red curve in figure 2a) which demarcates the carapace into anterior and posterior sides develops and gets more noticeable with growth and maturity of the tortoise.

This conclusion is reached from observation of carapaces of procured shells of various longitudinal sizes with the assumption that size rises with age. The rational reason for this age-dependent feature could be to create allowance for locomotion. This reason is based on two known morphological features;

1. The upper surface of the carapace is covered with hard keratinized scutes which gets harder with age.
2. The shell is naturally designed to deform at low levels of loading and stiffen at high levels of loading.

Counting from the nuchal, the hinge begins to develop at the sutural boundary between the 8th and 9thperipheral and grows into the sutural between the second and third carapacial plates. As the tortoise matures the hinges grows simultaneously from the two sides and finally merges at the middle line sutural boundary between the 3rd and 4th (counting from the anterior). At full level of maturity the carapacialplates is fully demarcated by the hinge. The fully developed hinges in figure 2(a) is indicated red.

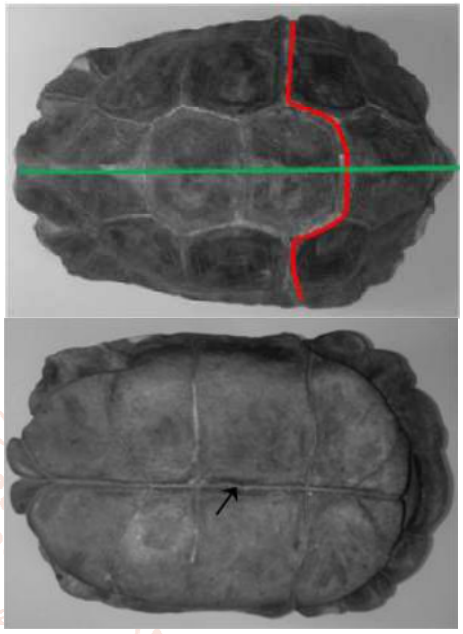

Figure 2. Picture of tortoise shell of the studied specie, (a) the dorsal view of the carapace indicating aline of symmetry (green) and (b) a ventral view of plastron indicating natural line of symmetry

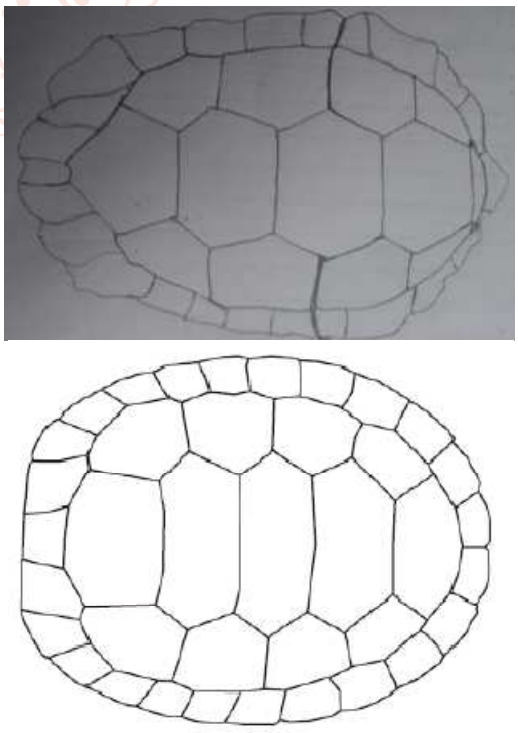

Figure 3. (a) A sketch of the dorsal view of carapace of the studied tortoise species and (b) A sketch ofcarapace of emydid turtle as adapted from the work [27].

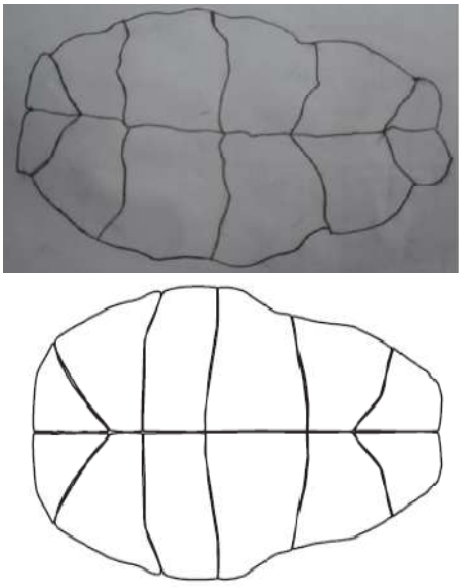

Figure 4. (a) A sketch of the ventral view of plastron of the studied tortoise specie and (b) A sketch ofplastron of emydid turtle as adapted from the work [27]4.4=5, 4.5=6,

3.1. Discussion of the Micro-structural results of the Shells

The microstructure of the studied shells was revealed with both optical microscope and scanning electron microscopy. Optical microscope was used to study the various parts of the saggital plane of a carapace. The results are presented in figures 5 and 6. The results in figure 5(a) are for the major parts of the carapace cross-section from the dorsal to the ventral parts. Keratin shown in figure 5(a) is the first major part from the dorsal direction. Indications of delaminations are seen in the keratin. The delaminations help the tortoise in dealing with shock loads by providing a mechanism for reduction of impulse and load dissipation. Next to the keratin is the dorsal cortex shown in figure 5(b). The dorsal cortex is seen to bedense and not to have any visible delamination. This is an indication that it is a load bearing member that is particularly evolved in the tortoise to resist dead load. Next to the dorsal cortex is the middle porous layer shown in figure 5(c). The middle porous layer is seen to have porosity. The porosity of the middle layer makes the carapace a sandwich composite with favourable stiffness to mass ratio. This porosity ensures that the carapace is not too heavy for the tortoise to carry thus simultaneously guarantees ease of locomotion and strength. The porosity of the middle layer also plays a major role in dissipation of impact loads. The ventral cortex is shown in figure 5(d). It completes the sandwich composite structure and resists tensile loads induced by compressive loads on the dorsal surface. The suture is the junction between two carapacial plates. It is shown in figure 6 to contain a zigzag interlocking design between adjacent plates. The suture is basically unmineralized collagen structure that allows slight deformation of the shell under light loads required for respiration, locomotion and metabolism. On application of heavy loads the bony zigzag edges of the adjacent plates become interlocked thus resisting excessive deformation.

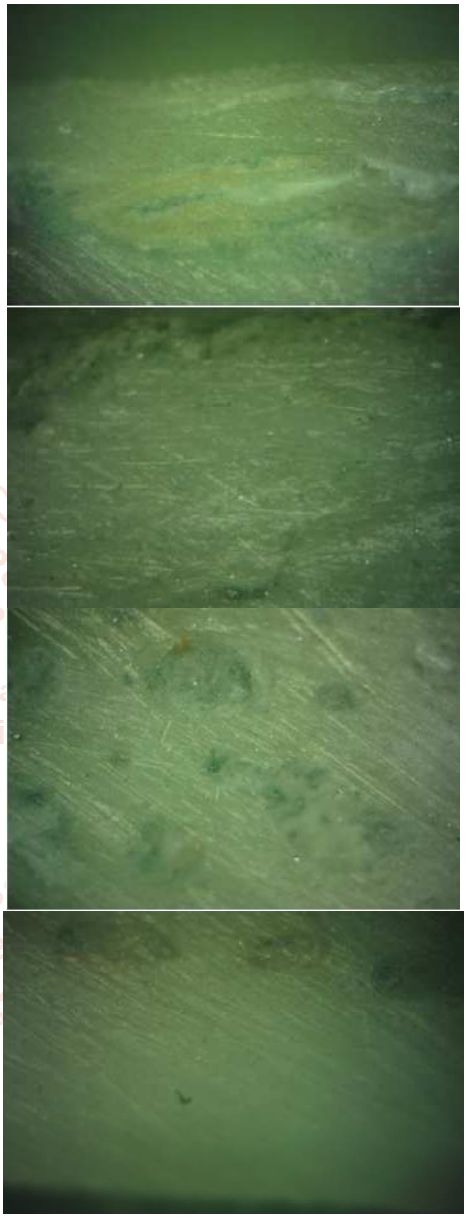

Figure 5. (a) Keratin with indications of delamination, (b) Dorsal cortex, (c) Middle porous layer, (d) theventral cortex

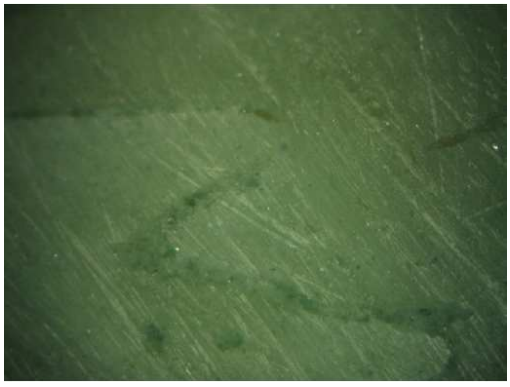

Figure 6. Suture with zigzag inter-locking design

3.2. Discussion of the whole-shell compression results

Two mature specimens were tested with the universal testing machine stationed at the Standards Organization of Nigeria (SON) Enugu. The results are presented in figure 7. The load deformation relationship shows a falling zigzag pattern. This could be due to the nature of the shell which allows theneighbourhood of the point of contact of carapace and the upper jaw of the machine to collapse followed by elastic response of the lower portions of the shell which has not collapsed.

This process is repeated with smaller peaks until the shell fails completely. It is noteworthy that the second peak is the highest in the two specimens. The specimen with the load-deformation diagram in figure 7 (a) has a mass of 0.2362kg while the mass for the specimen with the load-deformation diagram in figure 7 (b) is 0.2764Kg. The elastic constant (stiffness) of the initial linear portion of the two graphs is given by

$$k = \frac{F_f - F_i}{\delta_f - \delta_i}\ \frac{\Delta F}{\Delta \delta} \qquad (13)$$

The subscripts "i" and "f" respectively connotes initial and final values. It is seen from figure 7 (a) that $F_f = 3.7440\,KN$ and $F_i = 0.39\,KN$. Also it is seen from figure 7(a) that $\delta_f = 2.25mm$ and $\delta_i = 0mm$.

By making use of equation (13) the stiffness becomes $k = 1.4907\times10^{6}\,Nm^{-1}$

For the shell with mass0.2764Kg with load-deformation diagram represented in figure 7(b); $F_f = 3.0888KN$ and $F_i = 0KN$. Also it is seen from figure 7(a) that $\delta_f = 2.75mm$ and $\delta_i = 0mm$. By making use of equation (13) the stiffness becomes. $k = 1.1232\times10^{6}\,Nm^{-1}$

This stiffness values are high when compared with that of Trachemysscripta (red-ear turtle) of about $0.3125\times10^{6}\,Nm^{-1}kg^{-1}$ [12] as read from figure 7(c). This confirms one of the expectations that tortoise shell should be stiffer than those of turtle. It must be noted that the stiffness to mass ratio (k/m) for the two shells are respectively given by $6.3112\times10^{6}\,Nm^{-1}kg^{-1}$ and $4.0637\times10^{6}\,Nm^{-1}kg^{-1}$.

These k and F_f values will be utilized subsequently in computation of equivalent synthetic dooms for comparison with the above stiffness to mass ratios.

The SEM image of the failed surfaces of carapace and plastron are shown in figure 8. Figure 8(a) shows the failed surface of the carapace while figure 8(b) shows the failed surface of the plastron. It is seen from SEM image of the surfaces that the failed surfaces are rough indicating pullout of fibres. This deduction is based on comparison with SEM image of equal magnification of smoothly cut carapace in figure 8(c) which is seen to be relatively smoother than figure 8(a).

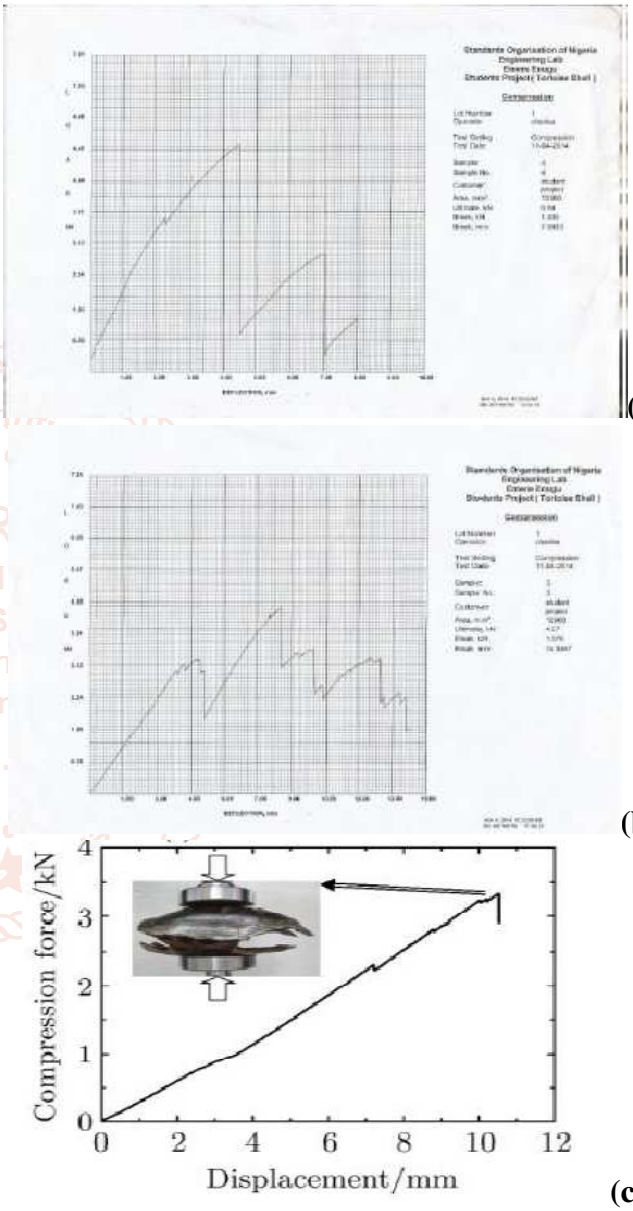

(a) (b) (c)

Figure 7. (a and b) The load deformation relationship in whole-shell compression test, (c) The load deformation relationship in whole-shell compression test of Trachemysscripta (red-ear turtle) [12]

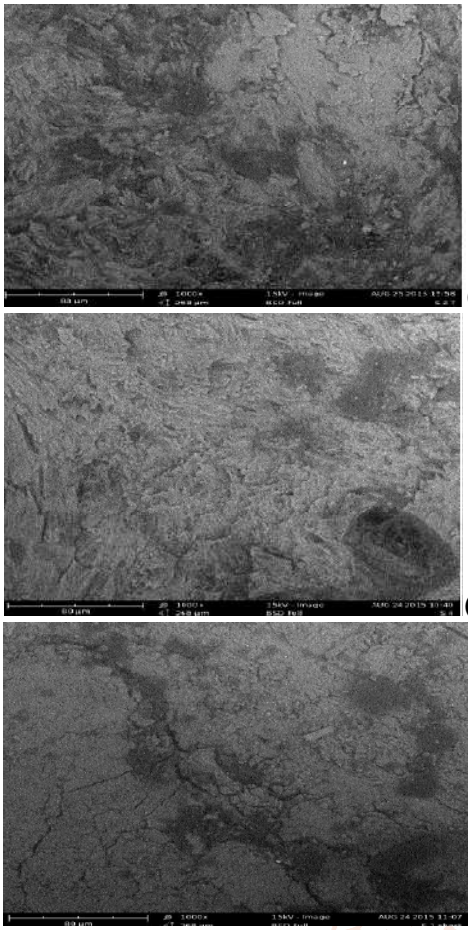

Figure 8. The SEM images of the failed surfaces of (a) carapace and (b) plastron, (c) The SEM images of the smoothly cut surface of carapace.

3.3. Discussion of the porosity tests

Since porosity is an important property of the shell as a multi-scale sandwich composite, it tested for the shell using the SEM. Figure 9 is a SEM image of saggital cross-section of carapacial specimen with indications of porosity and a plot of equivalent circle diameters of the pores as a function of the pore count. By summing the bars it is seen that there is a total of 133 Pores.

Analysis also indicates that Average porosity (Pore Area Ratio) of the image is 36.65%. The porosity analysis of the transverse crosssection of carapacial specimen gives average porosity of 28.97%. The average porosity of the failed transverse section of the carapace is 33.56%. The average porosity of the failed transverse section of the plastron is 24.99%. From the results of the four studied surfaces it can be said that the average porosity of the studied shell is 31.0425%. This figure for porosity is much smaller than the reported porosity of 48.9% for turtle Terrapene Carolina in the work [20].

This result is expected because the turtle requires more porosity in order to more effectively utilize the buoyant forces while swimming while the tortoise which is basically land dwelling requires denser and stronger shells to resist loads.

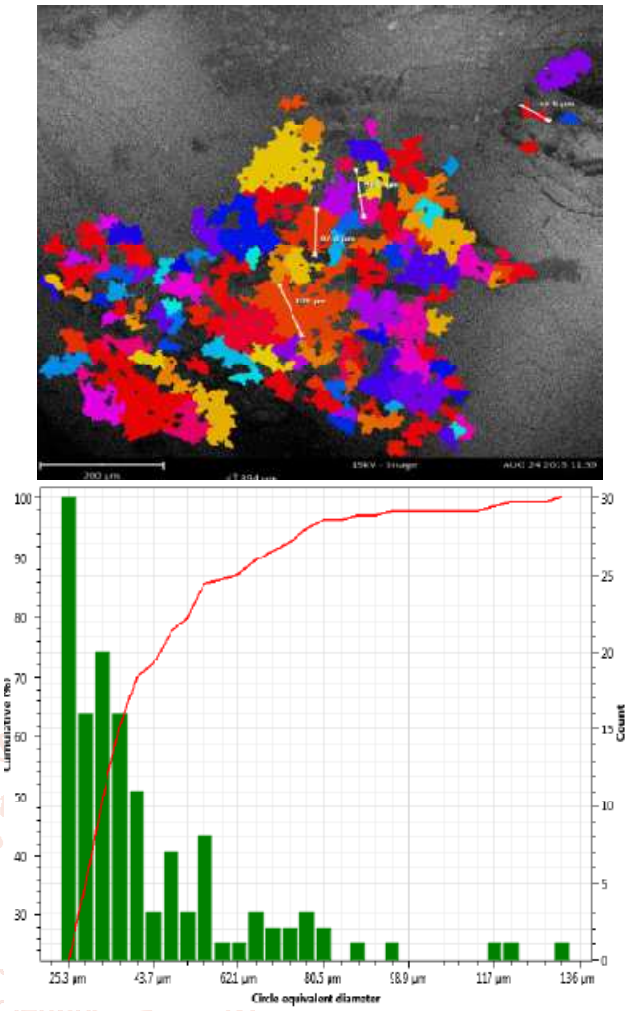

Figure 9. (a) SEM image of saggital cross-section of carapacial specimen with indications of porosity and (b) Plot of equivalent circle diameters of the pores as a function of the pore count.

3.4. Computation and Discussion of Equivalent Structural doom

Every other parameter in equation (12) is replaced with the parameters of the tortoise shell. Typical parameter values for emydid shell are $E_o = 1.07Gpa, v_0 = 0.31$, $d = 0.8$, $\theta = 0.310425, b = 0.95$ and $c = 1$[21]. The stiffness and failure force of the studied shells are seen from figure 7 to be

$k = 1.4907\times10^6 Nm^{-1}$ or $k = 1.1232\times10^6 Nm^{-1}$,

$F_f = 3.7440KN$ or $F_f = 3.0888KN$.

The thickness of the shells is $t = 3.0625mm$. These parameters are inserted in equation (12) and solved with MATLAB solution search function to give $D = 5mm$ and $5.5mm$ for the shells with load-deformation diagrams in figure 7(a) and figure 7(b) respectively.

It is seen that the diameters and of equivalent dooms of the shells with load-deformation diagrams in figure 7 are less than double of the thickness

$t = 3.0625mm$. This means that the calculated equivalent dooms are solid hemi-spheres and potentially of very high mass to stiffness ratio. The condition that mass to stiffness ratio of the tortoise shells should be higher than those of the equivalent synthetic dooms would require the density of the equivalent synthetic dooms to obey the inequality

$$\rho \rangle \frac{12m_{sh}}{D^3} \qquad (14)$$

Equation (14) gives the conditions $\rho \rangle 7.2177\times10^6 kgm^{-3}$ and $\rho \rangle 6.3457\times10^6 kgm^{-3}$ for the equivalent dooms of the shells with load-deformation diagrams in figure 7 to have higher stiffness to mass ratio. These densities are well beyond the range for normal metals. This means that the equivalent dooms made of normal metals will have higher stiffness to mass ratio than the studied tortoise shells.

This result can be explained if it is realized that the equivalent dooms in this case are solid isotropic delaminations in the biological shells are weak features of the composite system. The interlocking designat the sutures are points of stress concentration because at application of large loads the sharp tips of adjacent plates interlock and create points of stress concentration. This is why tortoise /turtle shells normally fail from the suture as observed for the studied biological system.

4. Conclusion

The macro-structural properties, micro-structural properties and mechanical properties of shells of tortoise of Easthern Nigeria extraction were studied experimentally. Comparing the shell of the studied specie with that of emydid turtle studied in literature led to identification of minor anatomical difference. The main difference between the two is that the most anterior and the most posterior plates are smaller in size relative to other plastral plates in the studied plastron than in the plastron of the emydid turtle.

Examination of the shell carapacial thickness under an optical microscope indicated that it is a natural sandwich composite made of keratin, dorsal cortex, porous bone and ventral cortex. Indications of delaminations which help the tortoise in dealing with shocks were seen in the keratin. The dorsal cortex was seen to be is a load bearing member with random distribution of fibers that has particularly evolved in the tortoise to resist dead load. The porosity seen in the middle porous layer ensures that the carapace is not too heavy for the tortoise to carry thus guarantees ease of locomotion, strength and damping. The ventral cortex helps to resist tensile loads induced by compressive loads on the dorsal surface.

The suture is the junction between two plates which was revealed to house zigzag interlocking design between adjacent plates. The revealed suture conforms to the knowledge that shells of testudines are naturally designed to allow slight deformation of the shell under light loads required for respiration, locomotion and metabolism but stiffen under excessive deformation.

Two mature shells were subjected to whole shell compression tests. The stiffness of the specimens were determined to be $k = 1.4907\times10^6 Nm^{-1}$ and $k = 1.1232\times10^6 Nm^{-1}$ for the shells with masses 0.2362 kg and 0.2764Kg respectively. These stiffness values were as expected higher the typical values for those of turtle. The stiffness to mass ratio (k/m) for the two shells were respectively calculated to be $6.3112\times10^6 Nm^{-1}kg^{-1}$ and $4.0637\times10^6 Nm^{-1}kg^{-1}$.

Analysis of four SEM surfaces revealed that average porosity of the studied shells is 31.0425%. This figure for porosity is as expected smaller than the value 48.9% reported for porosity of shell of the turtle Terrapene Carolina in literature. The expectation is based on the fact that the water dwelling turtles require more effective utilization of the buoyant forces for swimming while the tortoise which is basically land dwelling requires denser and stronger shells to resist loads. Based on the studied shells the conditions established for equivalent synthetic shells to have less mass to stiffness ratio are the $\rho \rangle 7.2177\times10^6 kgm^{-3}$ and $\rho \rangle 6.3457\times10^6 kgm^{-3}$ respectively. These densities are well beyond the range for normal metals meaning that the equivalent dooms have higher stiffness to mass ratio than the studied tortoise shells. The reason is that the equivalent dooms in this case are solid isotropic hemispheres while the tortoise shells are composed of plates joined at the sutures creating room for stress concentration and weakness at the joints. This explained why tortoise /turtle shells normally fail from the suture as observed for the studied biological system.

Reference

[1] Rieppel O, Reisz R R. The origin and early evolution of turtles. *Annual Review of Ecology and Systematics*, 1999, 30, 1–22.

[2] Burke A C. The development and evolution of the turtle body plan: Inferring intrinsic aspects of the evolutionary process from

experimental embryology. *American Zoologist*, 1991, 31, 616–627.

[3] Lee M S Y. Correelated progression and origin of turtles. *Nature*, 1996, 379, 811–815.

[4] Zangerl 1969] R. Zangerl, "The turtle shell", pp. 311–339 in Biology of the reptilia, edited by C. Gans, Academic Press, London, 1969.

[5] Heithaus, M. R., et al., 2008. A review of lethal and non-lethal effects of predators on adult marine turtles. Journal of Experimental Marine Biology and Ecology 356, 43–51.

[6] J. W. Gibbons, "Why do turtles live so long?", Biosci. 37: 4 (1987), 262–269.

[7] W. I. Boarman, "Managing a subsidized predator population: reducing common raven predation on desert tortoises", Environ. Manag. 32: 2 (2003), 205–217.

[8] K. Carpenter and D. Lindsey, "The dentary of Brachychampsamontana Gilmore. Alligatorinae; Crocodylidae/, a late Cretaceous turtle-eating alligator", J. Paleontol. 54: 6 (1980), 1213–1217.

[9] G. Pérez-Higareda, A. Rangel-Rangel, H. M. Smith, and D. Chiszar, "Comments on the food and feeding habits of Morelet's crocodile", Copeia 1989: 4 (1989), 1039–1041.

[10] S. E. Stancyk, "Non-human predators of sea turtles and their control", pp. 139–152 in Biology and conservation of sea turtles: proceedings of the World Conference on Sea Turtle Conservation (Washington, DC, 1979),

[11] L. H. David, K. Sielert, M. Gordon, Turtle Shell And Mammal Skull Resistance To Fracture Due To Predator Bites And Ground Impact, Journal Of Mechanics Of Materials And Structures, 6, (9- 10), 2011.

[12] W. Zhang, C. Wu, C. Zhang and Z Chen. Microstructure and mechanical property of turtle shell, Theoretical & Applied Mechanics Letters 2, 014009 (2012)

[13] W. Zhang, C. Wu, C. Zhang, Z. Chen, Numerical Study of the Mechanical Response of Turtle Shell, Journal of Bionic Engineering 9 (2012) 330–335.

[14] D C., Jackson. How a turtle's shell helps it survive prolonged anoxic acidosis. *News in Physiological Sciences*, 15**,** (2000) 181–185.

[15] Gilbert, S. F., et al., 2001. Morphogenesis of the turtle shell: the development of a novel structure in tetrapod evolution. Evolution & Development 3, 47–58.

[16] S. Krauss, E. Monsonego-Ornan, E. Zelzer, P. Fratzl, R. Shahar. Mechanical function of a complex three-dimensional suture joining the bony elements in the shell of the red-eared slider turtle. Advanced Materials 21, (2009) 407–412.

[17] ME. Rosenberg. Carapace and plastron sensitivity to touch and vibration in the tortoise (Testudohermanni and T. graeca). J ZoolLond 208 (1986) 443–455.

[18] K. Balania, R. R. Patelb, A. K. Keshrib, D. Lahirib, A. Agarwal, Multi-scale hierarchy of Chelydraserpentina: Microstructure and mechanical properties of turtle shell. Journal of the mechanical behaviour of biomedical materials 4 (2011) 1440–1451

[19] Wyneken, J., 2001. The Anatomy of Sea Turtles. US Department of Commerce NOAA Technical Memorandum NMFS-SEFSC-470.

[20] H. Rhee a, M. F. Horstemeyer, Y. Hwang, H. Lim, H. El Kadiri, W. Trima, A study on the structure and mechanical behaviour of the Terrapenecarolina carapace: A pathway to design bioinspiredsynthetic composites, Materials Science and Engineering, 29 (2009) 2333–2339

[21] R. Damiens, H. Rhee, Y. Hwang, S. J. Park, Y. Hammi, H. Lim, M. F. Horstemeyer, compressive behavior of a turtle's shell: experiment, Modeling, and simulation, journal of the mechanical behavour of biomedical materials 6 (2 0 1 2) 1 0 6 – 1 1 2

[22] Lv, S., et al., 2010. Designed biomaterials to mimic the mechanical properties of muscles. Nature 465, 69–73.

[23] Xia, F., Jiang, L., 2008. Bio-inspired, smart, multiscale interfacial materials. Advanced Materials 20, 2842–2858.

[24] C. R. Steele, Asymptotic analysis and computation for shells, pp. 3–31 in Analytical and computation models of shells, edited by A. K. Noor et al., ASME, New York, 1989

[25] Panakkal, J. P., Willems, H., Arnold, W., 1990. Non-destructive evaluation of elastic parameters of sintered iron powder compacts. J. Mater. Sci. 25, 1397–1402.

[26] Gibson, L. J., Ashby, M. F., 1997. Cellular Solids: Structure and Properties, second ed. Cambridge University Press, Cambridge, U. K.

[27] P. M. Magwene, J. J. Socha. Biomechanics of turtle shells: How whole shells fail in compression. J. Exp. Zool. (2012) 9999A: 1–13.